

Changes in the subsurface stratification of the Sun with the 11-year activity cycle

S. Lefebvre¹

Physics and Astronomy Building, UCLA, Los Angeles, CA 90095-1547, USA

lefebvre@astro.ucla.edu

and

A. G. Kosovichev²

W. W. Hansen Experimental Physics Laboratory, Stanford University, Stanford, CA 94305-4085, USA

ABSTRACT

We report on the changes of the Sun’s subsurface stratification inferred from helioseismology data. Using SOHO/MDI (Solar and Heliospheric Observatory/Michelson Doppler Imager) data for the last 9 years and, more precisely, the temporal variation of f-mode frequencies, we have computed the variation of the radius of subsurface layers of the Sun by applying helioseismic inversions. We have found a variability of the “helioseismic” radius in antiphase with the solar activity, with the strongest variations of the stratification being just below the surface around $0.995R_{\odot}$. Besides, the radius of the deeper layers of the Sun, between $0.975R_{\odot}$ and $0.99R_{\odot}$ changes in phase with the 11-year cycle.

Subject headings: Sun: helioseismology — Sun: oscillations — Sun: activity — Sun: interior

1. Introduction

For the last decades, temporal variations in the solar radius has been a controversial subject. Indeed, measurements made with the solar astrolabe by F. Laclare in France (Laclare et al. 1996) and the Brazilian team (Reis Neto et al. 2003) showed a variation of the solar radius in antiphase with the solar activity cycle, while F. Noël in Chile (Noël 2004) using a similar instrument reported a variation in phase with the solar activity. By using

solar continuum intensity images obtained with the Michelson Doppler Imager (MDI) on board SOHO, Emilio et al. (2000) found a variation of the solar radius of 8.1 ± 0.9 mas/yr, but in a recent and more complete study of these images, Kuhn et al. (2004) reported no evidence of solar-cycle visible radius variations between 1996 and 2004 at any level above 7 milliarcseconds: this is significantly lower than any variation reported from ground-based observations. Other measurements made by the Solar Disk Sextant (SDS) experiment on-board stratospheric balloons (Sofia et al. 1994; Thuillier et al. 2005) reported a variation of the solar radius in antiphase with the solar radius. The solar radius can be also determined by helioseismic methods (Schou et al. 1997). This, so-called “seismic” radius, is related to the subsurface density stratification and can be compared with the “photospheric” radius, as inferred by astrolabe ground-based measurements, for example, only by using solar models. The “seismic” radius probes the sub-photospheric layers up to a depth of about 15 Mm. So the use of solar f-mode frequencies to infer the seismic radius is important for searching for physical changes occurring beneath the photosphere. Results are, however, conflicting. Dziembowski et al. (2001) reported rates of the seismic radius change ranging from -3 to 1 km/year during the rise of cycle 23. Recently, Dziembowski & Goode (2005) reexamined the issue by using SOHO/MDI f modes for 1996-2004, and were unable to obtain stable results for the seismic radius, and thus they concluded that the observed variations of the f-mode frequencies should be explained by the direct effect of magnetic field. However this led to unrealistically strong random field hidden below the surface. So, the question whether or not there is a radius variation with the activity cycle is still debated. Moreover if there are such variations at the surface, where is their origin? In this letter, we consider the issue of solar radius and determine solar radius variations with time for various layers below the surface. The main difference from the previous investigations is that we do not assume an uniform change of the radius of subsurface layers, but allow variations of displacement of these layers with depth. We show that a stable solution does exist in this case, and find evidence for temporal solar radius variations in the sub-photospheric layers above $0.97R_{\odot}$ with an oscillation, in antiphase with the solar cycle above $0.99R_{\odot}$ and in phase below. Our results show the localization of these variations in the upper convective zone. If we extrapolate these results up to the surface, we find a radius change of about 2 km in antiphase with the solar cycle: here, we have to keep in mind that without high-l, we cannot constrain the surface radius better, and that in reality, this variation at the surface can be larger provided it is more localized.

2. Data

We used frequencies of solar oscillation modes from 72-day MDI observing runs, computed by J. Schou¹. We selected only f modes for the observing period 1996-2004. Each file has a different number of f modes, so we extracted only common modes from these files and obtained a total of 151 modes ranging from the angular degree $l = 125$ to $l = 285$. We have computed the relative frequency changes $\delta\nu/\nu$ for each degree and calculated the average over each year and binned every 20 μHz . The reference year has been chosen to be 1996, near the minimum of the solar cycle². The averaging over 1-year of the data allowed us to avoid the instrumental 1-year variations. The results are compiled on Fig. 1. The errorbars are not plotted for clarity of the graph.

The different curves plotted on this figure shows an evidence of variations in the f-mode frequencies over the solar cycle already pointed out by Dziembowski et al. (2001). We emphasize an intriguing phenomenon at higher l , above $\nu = 1600 \mu\text{Hz}$, where the frequency difference can change of sign, becoming then negative, in the descending part of the solar cycle. It is particularly puzzling that the sharp frequency decrease above 1600 μHz continues in the declining phase of the solar cycle whereas the frequencies of the lower-frequency modes return to their previous solar minimum values. We don't know how to interpret this change but assume that it may come from a variation in the near-surface turbulence, which can affect the frequencies of the f modes confined just below the surface, in a zone close to the leptocline (from the greek *leptos*=fine), thin transition layer between the upper convective zone and the photosphere (Godier & Rozelot 2001; Rozelot & Lefebvre 2003). We used these computed frequency differences (without the binning over ν) between $l = 150$ and 250, which are measured most reliably, as input parameters in our helioseismic inversion presented in the next section.

3. Helioseismic inversion of f modes to infer solar radius variations

3.1. Mathematical formalism

As a starting point for our inversion, we used the equation derived by Dziembowski & Goode (2004) who established a relation between the relative frequency variations $\delta\nu/\nu$ for f-mode frequencies and the associated Lagrangian perturbation of the radius $\delta r/r$ of

¹<http://quake.stanford.edu/~schou/anavw72z/>

²For this year, data begin from May 1st.

subsurface layers:

$$\left(\frac{\delta\nu}{\nu}\right)_l = -\frac{3l}{2\omega^2 I} \int dI \frac{g}{r} \frac{\delta r}{r} \quad (1)$$

where l is the degree of the f modes, I is the moment of inertia, ω the eigenfrequency and g the gravity acceleration.

This equation leads to the asymptotic relation used in the previous determinations of the solar radius using f modes $\frac{\Delta\nu_l}{\nu_l} = -\frac{3}{2} \frac{\Delta R_\odot}{R_\odot}$ (Schou et al. 1997), assuming that $\frac{\delta r}{r}$ is constant with depth. However, we don't make this assumption, and infer $\frac{\delta r}{r}$ as a function of r . Eq. 1 can be rewritten as

$$\left(\frac{\delta\nu}{\nu}\right)_l = \int_0^{R_\odot} K_l \frac{\delta r}{r} dr \quad (2)$$

where the kernel K_l is expressed as

$$K_l = -\frac{3l}{2\omega_l^2 I_l} \rho \left| \vec{\xi}_l \right|^2 gr \quad (3)$$

ρ being the density and $\vec{\xi}_l$ the mode eigenfunction.

To compute each kernel K_l , we used the model S (Christensen-Dalsgaard et al. 1996) calibrated to the seismic radius of Schou et al. (1997) ($R_\odot = 6.9568 \times 10^5$ km). Fig. 2 shows three examples of the kernels at $l = 150, 200$ and 250 . The method used to invert Eq. 2 is the standard Regularised Least-Square technique (Tikhonov & Arsenin 1977), appropriate for this kind of ill-posed problems. In this method, one has to minimize the following relation

$$\begin{aligned} E &= \sum_l \frac{1}{\sigma_l^2} \left(\int_0^{R_\odot} K_l y dr - f_l \right)^2 + \alpha \int_0^{R_\odot} y^2 dr \\ &+ \beta \int_0^{R_\odot} \left(\frac{dy}{dr} \right)^2 dr \end{aligned} \quad (4)$$

where $y = \frac{\delta r}{r}$, $f_l = \left(\frac{\delta\nu}{\nu}\right)_l$, σ_l the relative uncertainty for each f_l , α and β the regularisation parameters.

3.2. Results

In the inversion process, we restricted the data set using only modes with l ranging from 150 to 250 measured more accurately than the other modes. For each year, the minimization of Eq. 4 leads to a solution plotted on Fig. 3. This solution integrated through Eq. 2 yields the relative frequencies variations versus the degree l in comparison with the real data. The

reconstructed frequencies fit pretty well the trend of the real relative frequencies within the errorbars (Fig. 4). Fig. 5 shows the ΔR estimated at the surface using $R_{\odot} = 6.9568 \times 10^5$ km as a reference in the model. Fig. 6 shows the averaging kernels (Ory & Pratt 1995) which illustrate the resolving power of these inversions. It is quite clear that the spatial resolution (FWHM) is about $0.005R_{\odot}$ in the region between $0.98R_{\odot}$ and $0.998R_{\odot}$. Like in other inverse problems, this means that the variations of the smaller scale and outside this region cannot be resolved without additional constraints. In Fig. 7 we give three examples of test inversions with artificial f-mode frequency data (applying the observed error estimates), which illustrate the accuracy and limitations of these inversions.

The main characteristics of our solution are:

1. Fig. 3 shows no significant changes in the variation of the subsurface layers depth below $0.97R_{\odot}$. In this layers, our inversions loose the spatial resolution as follows from Fig. 6. So, with the currently available data, it is not possible to measure localized variations below $0.97R_{\odot}$. However, if there were an uniform change of the radius in subsurface layers (including $0.97R_{\odot}$ and below) of the order of 1-3 km as discussed by Dziembowski et al. (2001), it could be detected by the inversion procedure as illustrated in the top panel of Fig.7 (no assumption was made about the functional form of the solution).
2. Fig. 3 shows non-monotonic changes in the stratification with the inner layer (below $0.99R_{\odot}$) moving up during the increase of activity (compression) and the outer layer (above $0.99R_{\odot}$) moving down (relaxation). The precise localization of these layers is uncertain because have a characteristic width of about $0.005R_{\odot}$. The test inversion in Fig.7 (middle panel) shows that this uncertainty can be about the half-width of the averaging kernels, about $0.003R_{\odot}$.
3. Fig. 5 estimates that the near-surface variations are in antiphase with the solar cycle with an amplitude of the order of 2 km. However, the sensitivity of our inversions is quite low at the surface, and localized variations of the surface radius may not be detected (see a test inversion in bottom panel of Fig.7). High-degree f-mode data are required to improved the surface estimates.

Note that if we used all the modes available (i.e. 151 modes), we cannot find a stable solution that fits the last part of the curves above $\nu = 1600 \mu\text{Hz}$ (see Fig. 1). We suppose that the behavior of the curves in this range of frequencies could be due to the influence of turbulence and magnetic fields very near the surface.

4. Discussion

First of all, Fig. 3 shows a temporal variation of the solar radius in the subsurface layers during the solar cycle. This oscillation is centered around $r = 0.99R_{\odot}$ with a width of about $0.03R_{\odot}$. This anomaly is composed of two parts: the first, below $r = 0.99R_{\odot}$, is in phase with the solar cycle and has a maximal amplitude of about 10 km; the second part above $r = 0.99R_{\odot}$, is in antiphase with the solar cycle and reaches larger amplitudes, of about 26 km. These variations indicate the presence of a changing with the solar cycle of a physical structure that could be described as a very thin transition layer, siege of the variation of the solar radius. This transition layer is located here approximately at $0.99R_{\odot}$ and it is linked to changes in the upper convective zone caused by magnetic fields. We estimate a variation of the seismic radius at the surface of about 2 km at the maximum of the cycle 23. However, the surface radius is poorly constraint with the currently available set of medium-l f-mode frequencies.

Our helioseismic inversion computations have put in evidence a variability of the solar radius in the subsurface layers which are extended to the surface. The results are generally consistent with previous conclusions that solar-cycle variations in the solar radius are confined to the outermost layers of the Sun (Antia & Basu 2004; Dziembowski & Goode 2005). This variability is localized in a double-structure layer centered at $0.99R_{\odot}$: in the deeper part, between $0.97R_{\odot}$ and $0.99R_{\odot}$, the radius varies in phase with the solar cycle, whereas this is opposite in the upper part above $0.99R_{\odot}$, where the variability become in antiphase. Thus we confirm the fact that the surface layers of the Sun are shrinking during the ascending phase of the solar cycle and is relaxing after the maximum. However, these changes are not uniform with depth. In a near future, it would be interesting to inspect more in details the behavior very close to the surface by looking at changes of the higher degree modes, above $l = 250$, where a second thin layer may take place.

As a conclusion, we would like to emphasize our most significant result: the change in radius goes from being in phase with the solar cycle in the deeper layers to out of phase in the shallower layers with a transition at $0.99R_{\odot}$. This result could eventually lead to a deeper understanding of the physics behind the changes.

This work utilizes data from SOHO/MDI and we thank J. Schou for providing the frequencies files.

REFERENCES

- Antia, H. M., & Basu, S. 2004, in ESA-SP 559, Proceedings of the SOHO 14 / GONG 2004 Workshop: Helio- and Asteroseismology: Towards a Golden Future, ed. D. Danesy, 301
- Christensen-Dalsgaard et al. 1996, *Science*, 272, 1286
- Dziembowski, W. A. et al., 2001, *ApJ*, 553, 897
- Dziembowski, W. A., & Goode, P. R. 2004, *ApJ*, 600, 464
- Dziembowski, W. A., & Goode, P. R. 2005, *ApJ*, 625, 548
- Emilio, M. et al., 2000, *ApJ*, 543, 1007
- Godier, S., & Rozelot, J. P. 2001, *Sol. Phys.*, 199, 217
- Kuhn, J. R. et al., 2004, *ApJ*, 613, 1241
- Laclare, F. et al., 1996, *Sol. Phys.*, 166, 211
- Noël, F. 2004, *A&A*, 413, 725
- Ory, J., & Pratt, R. G. 1995, *Inverse Problems*, 11, 397
- Reis Neto, E. et al., 2003, *Sol. Phys.*, 212(1), 7
- Rozelot, J. P., & Lefebvre, S. 2003, *Lecture Notes in Physics*, 599, 4
- Schou, J. et al., 1997, *ApJ*, 489, L197
- Sofia, S. et al., 1994, *ApJ*, 427, 1048
- Thuillier, G. et al., 2005, *Advances in Space Research*, 35, 329
- Tikhonov, A. N., & Arsenin, V. Y. 1977, *Solutions of ill-posed problems*, Washington D. C.: Winston

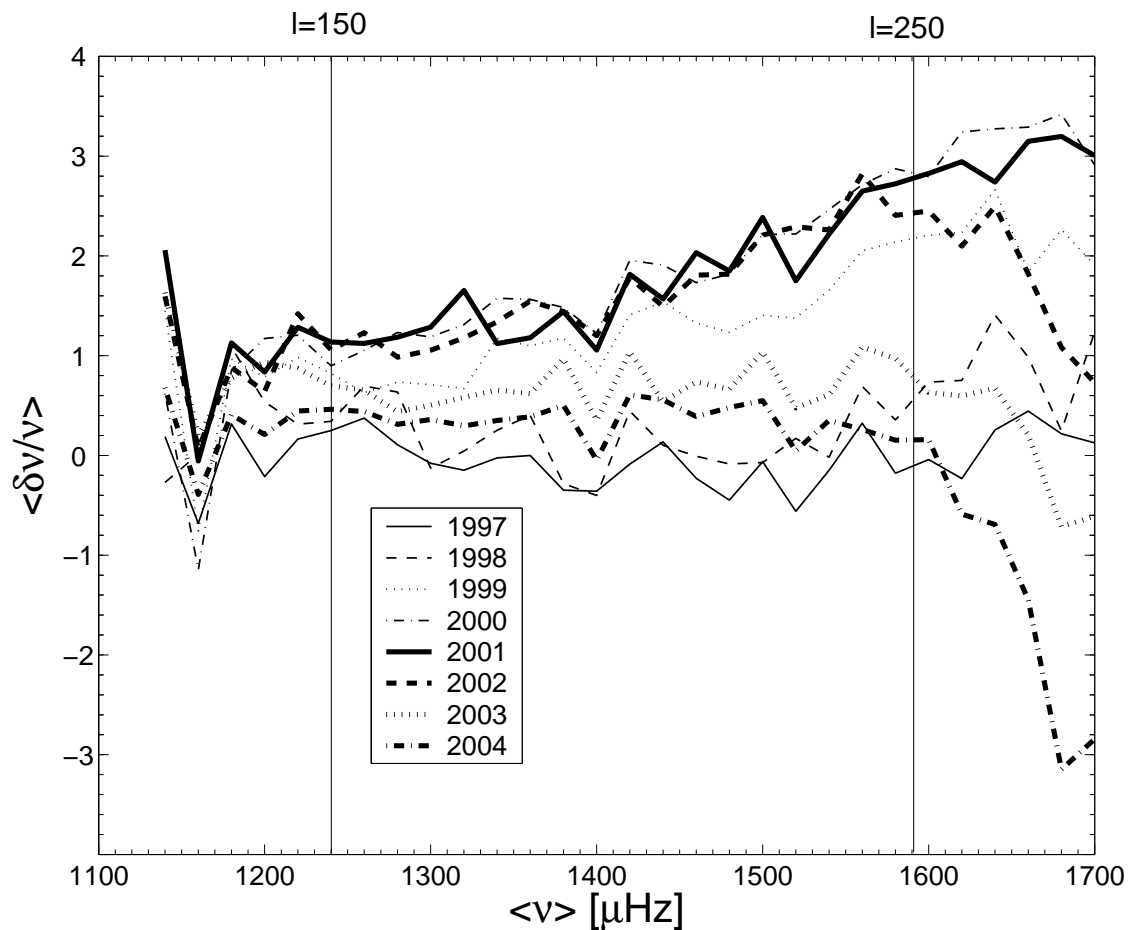


Fig. 1.— Average relative frequency differences in f-mode $\langle \delta\nu/\nu \rangle$ as a function of $\langle \nu \rangle$, average frequencies binned every $20 \mu\text{Hz}$. The reference year is 1996 and the errorbars have not been plotted for clarity of the graph. The f modes chosen for our study have frequencies between the limits represented by vertical lines.

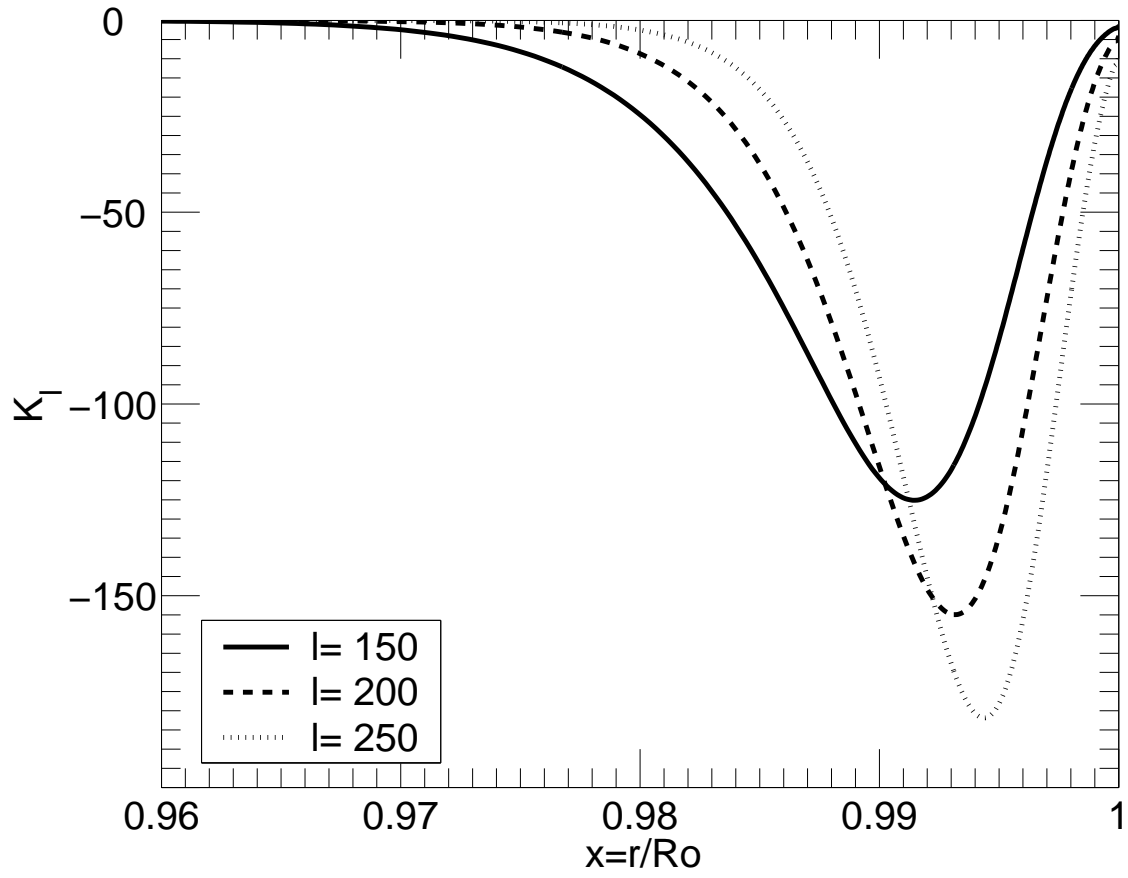


Fig. 2.— Example of kernels K_l at $l = 150, 200$ and 250 .

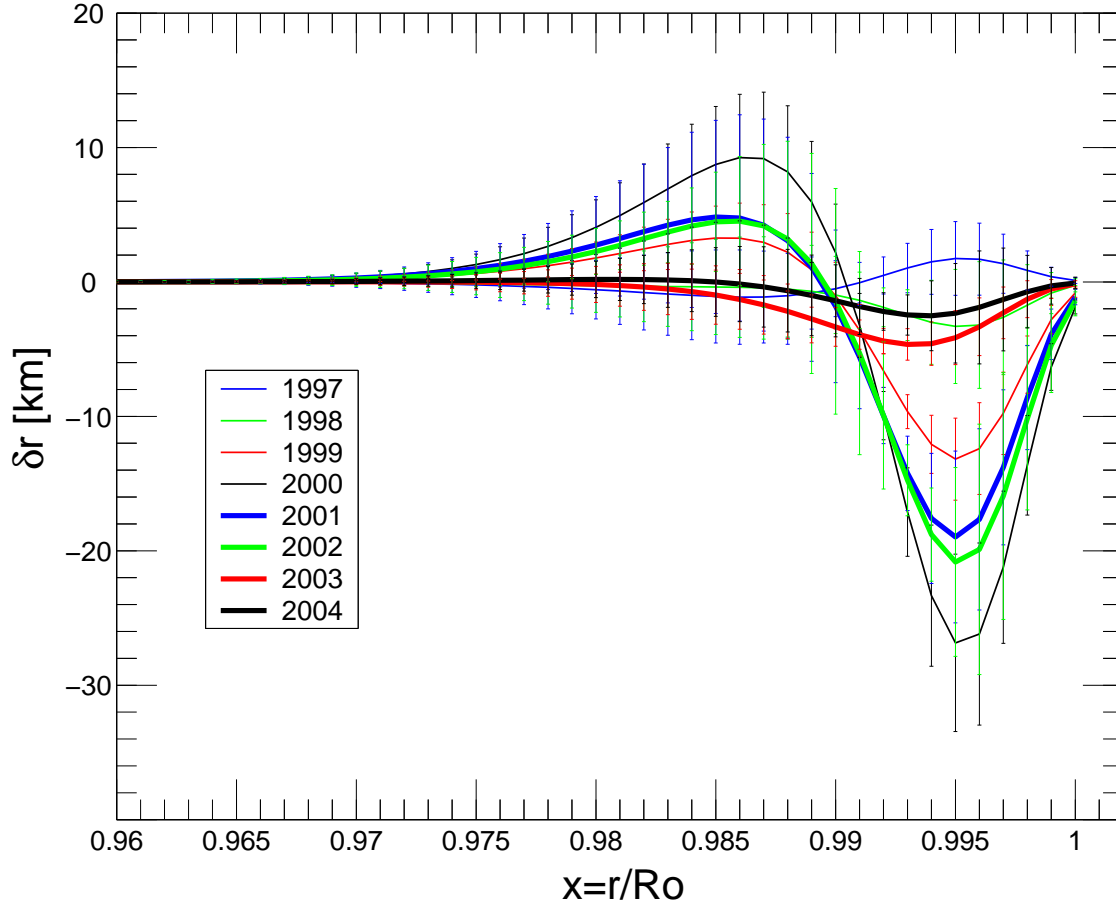


Fig. 3.— $\langle \delta r \rangle$ as a function of the fractional radius $x = r/R_\odot$, obtained as a solution of the minimization of Eq. 4. Notice the behavior of the curve near $x = 0.99$. The errors are the standard deviation after average over a set of random noise added to the relative frequencies reconstructed in Fig. 4.

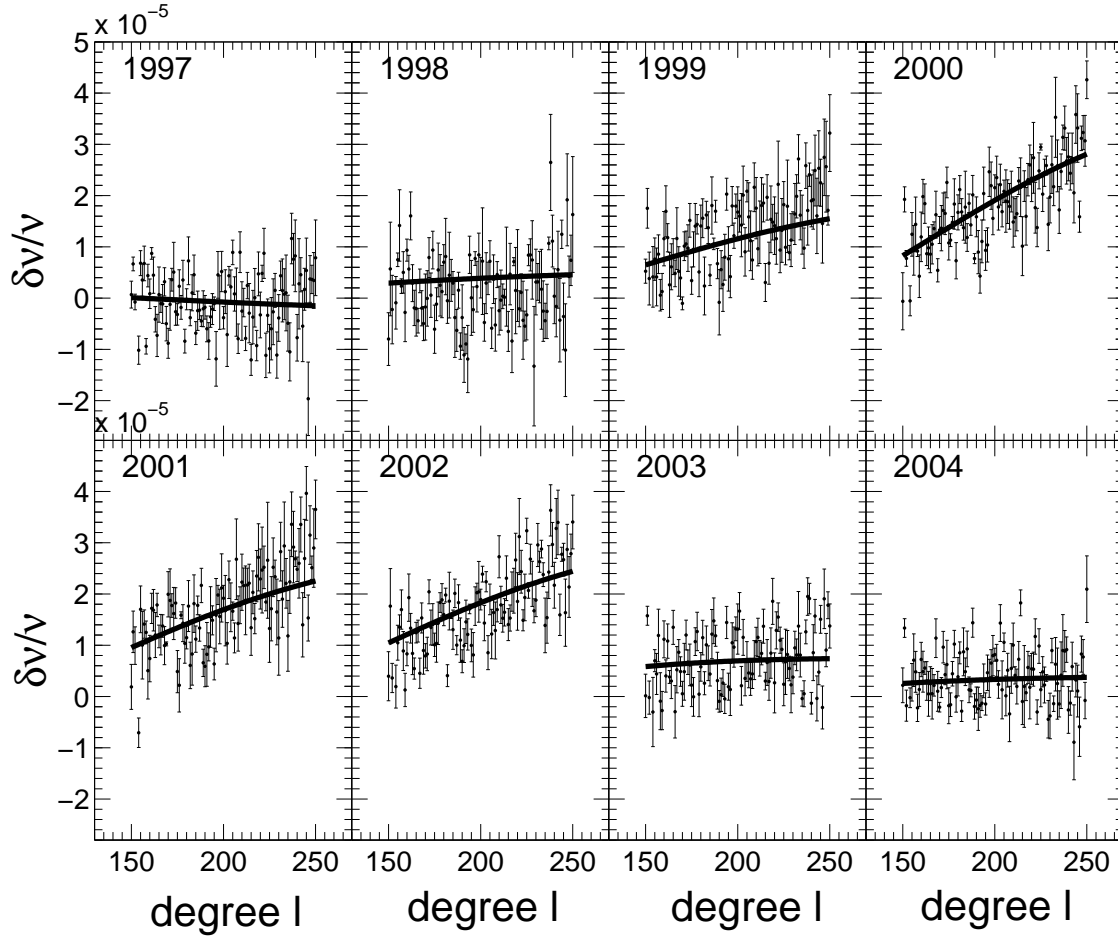


Fig. 4.— For each year, $\langle \delta\nu/\nu \rangle$ as a function of the degree l . The reference year is 1996 and the errors are the relative uncertainties. The solid curve is the results of direct integration of Eq. 2 providing the solution of Fig. 3.

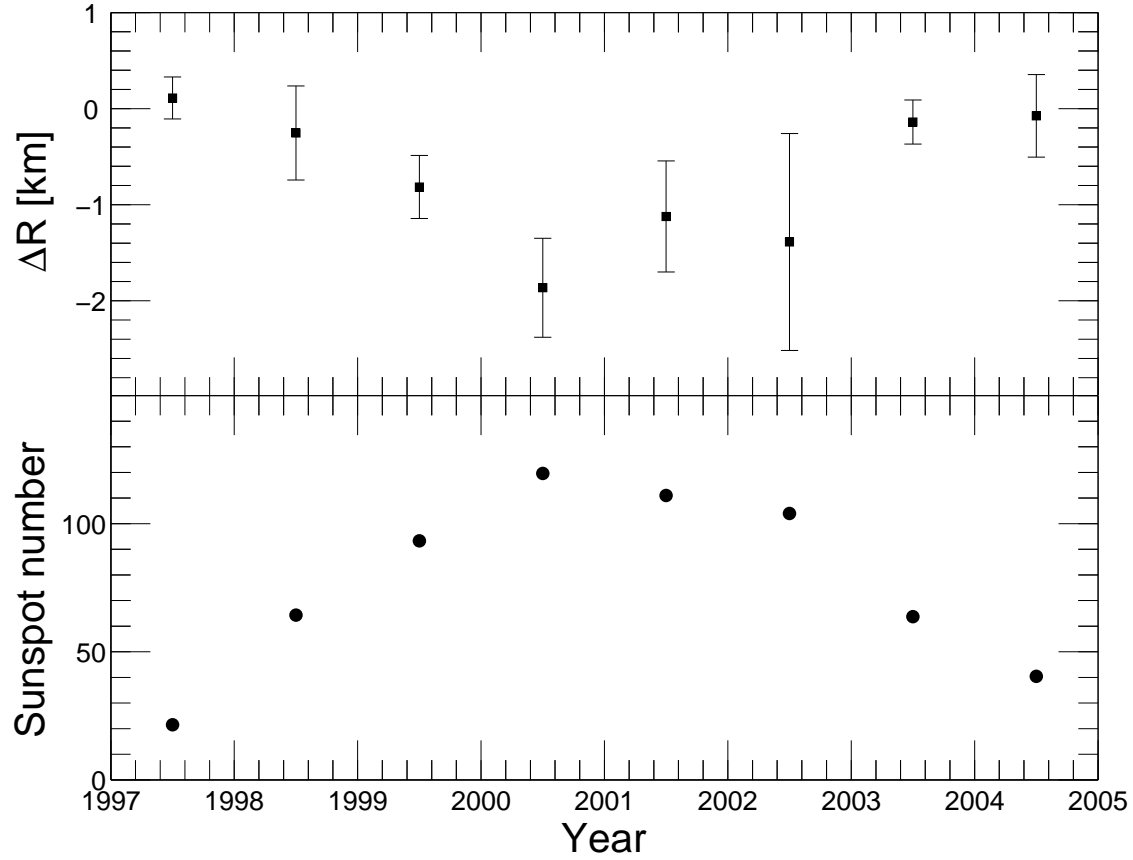


Fig. 5.— Top: temporal variation of ΔR near the solar surface at $r = R_{\odot}$ from the solution of Fig. 3. Bottom: Variation of the sunspot number for the same period. The variation of the seismic radius at the surface is found in antiphase with the solar cycle with an amplitude of about 2 km. It is important to keep in mind that without high- l , we cannot constrain the surface radius better, and that in reality, this variation at the surface can be larger provided it is more localized.

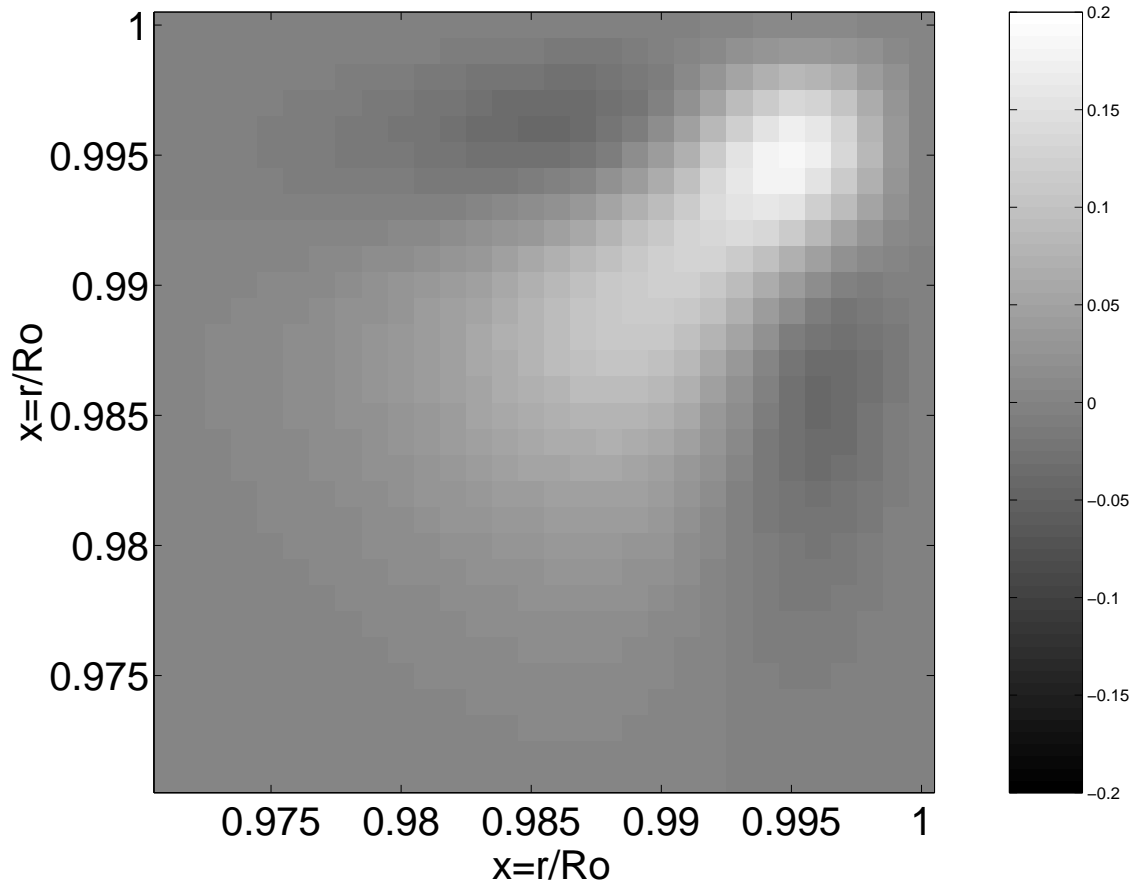


Fig. 6.— Amplitude of the averaging kernels versus the fractional radius x .

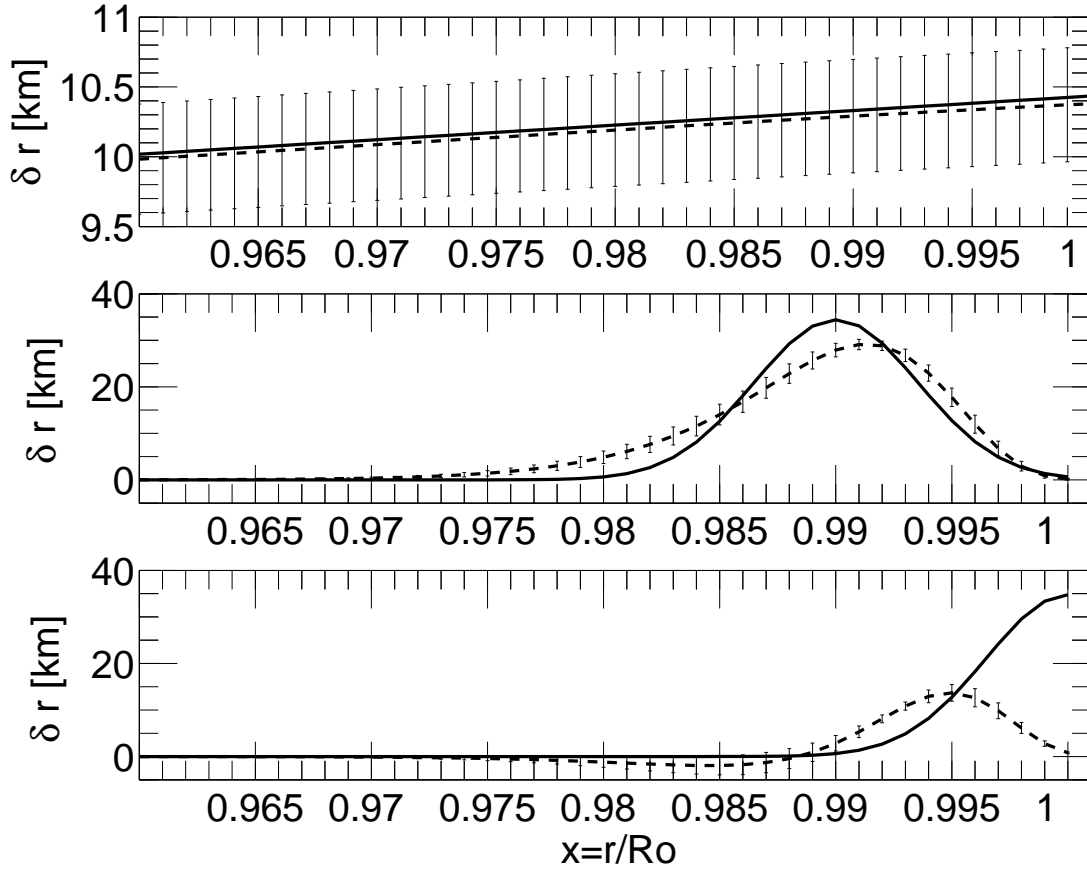


Fig. 7.— Inversion tests with artificial data; from top to bottom: the initial $\delta r/r$ is a constant, a gaussian with a width of 0.005 and centered on $x=0.99$, a gaussian with a width of 0.005 and centered on $x=1$. In all cases, the solid line is the initial data and the dashed curve is the result after inversion.